Current Distributions Governed by Coupled Concentration and Potential Fields

J. Deliang Yang and Alan C. West
Dept. of Chemical Engineering, Materials Science, and Mining Engineering, Columbia University, New York, NY 10027

Results from steady and unsteady, two-dimensional simulations of tertiary current distributions at and below the limiting current density are presented. The simulations are based on dilute-solution theory, with coupling of the concentrations of the ionic species through the electrical field. The electrical field is calculated from the electroneutrality constraint. Results confirm and extend previous theoretical predictions of the electrical-migration enhancement of the limiting current. To demonstrate the potential utility of general current-distribution solvers, measured temporal variations of the rate of copper deposition in the presence of an oscillating shear flow are measured and simulated. Experiments agree well with simulations.

Introduction

Electrochemical reaction rates often depend on both the electrical-potential difference between the electrode and adjacent solution and the surface concentration of at least one species. When the conditions are not ideal, nonuniform spatial distributions of the reaction rate arise. Simulations that estimate the degree of nonuniformity have become an important design tool, especially for metallization applications in the electronics industry (Dukovic, 1993). Normally, two limiting cases of current distribution phenomena are treated: in one case, nonuniformities due to concentration variations alone are considered, and in the other, nonuniformities due to electric-field effects alone are simulated.

The appropriateness of these asymptotic cases is explained by Newman (1991). In many practical situations, such as alloy deposition or deposition in the presence of additives, the current distribution may not clearly fall into either limiting case. Thus, it would seem useful to develop computational methodologies that eliminate hard-to-justify approximations. Specifically, it is necessary to solve for concentration fields and the potential field simultaneously. The solution to such problems is often termed the tertiary current distribution. Tertiary current distributions have not been treated extensively, especially when an analytic or semianalytic solution is infeasible.

Baker et al. (1991) and Pillay and Newman (1993) developed a method to transform the coupled transport equations to a single Laplace's equation. However, this method can only be used for problems with no convection and additional restrictive boundary conditions. Newman (1968, 1991) outlined a procedure valid under different conditions. His technique uses the fact that many flows of interest lead to boundary layers and that the Schmidt number for an ionic species in water is large. Concentration variations are thus restricted to a region near the electrode, allowing the separate treatment of the diffusion layer and the bulk region. In the bulk, the electrical potential is assumed to satisfy Laplace's equation, with a matching constraint that the current density calculated from ohm's law agrees with calculations within the diffusion layer. The procedure has been applied to disk (Newman, 1966; Vahdat and Newman, 1973; Law and Newman, 1986; Orazem and Miller, 1987), planar (Parish and Newman, 1969, 1970), and tubular (Alkire and Miraferi, 1973, 1977a,b; Pesco and Cheh, 1989) electrodes. The treatment of separate regions is restricted to flows that result in a thin diffusion layer. Often a more complicated flow field exists; for example, recirculation or boundary-layer separation may occur near cavities or protrusions on surfaces.

Alavyoon (1992) provided an example in which the coupled concentration and potential fields are solved throughout the entire computational domain along with natural-convection flow fields. Equations were solved by evaluating the nonlinear terms at the previous time step. Harb and Alkire (1991a,b) have modified FIDAP, a commercial fluid-flow solver (Engelman, 1986), to solve for a tertiary current distribution in a pit. However, few details of the numerical procedure were given.

The present investigation considers the tertiary current distribution on a line electrode in the presence of steady and unsteady shear flows. Calculations are performed with software based on a control-volume formulation. A previous theoretical treatment of the effect of migration on mass-transfer-limited currents is extended. Copper deposition was also studied experimentally to demonstrate the feasibility of using current-distribution solvers with data taken in one cell to predict behavior in other reactor configurations.

Theory

A diagram of the electrochemical cell is shown in Figure 1. The working electrode of length $2L$ is mounted on an otherwise insulating plate that oscillates in its own plane with frequency ω. The counterelectrode is placed a distance B from the working electrode. For microfabrication processes, it is common that $L/B \ll 1$. Therefore, the solution domain is essentially semi-infinite. (For a convection-diffusion problem, where the electrical potential is not relevant to the prediction of current distribution, a semi-infinite domain poses no conceptual problems; however, the treatment of an electrical potential in a two-dimensional, semi-infinite problem is problematic. When comparing simulation with experiment, the potential drop between the outer edge of the computational domain and the actual position of the reference or counterelectrode must be estimated.) The analysis of current distribution in this cell under conditions where electrical migration is unimportant was given previously (Wang et al., 1994; DeBecker et al., 1995a,b).

The electrical current in the solution is carried by ions. Assuming that the flux of ions is given by dilute-solution theory, the dimensionless flux of species j is

$$N_j = - z_j D_j c_j \nabla\Phi - D_j \nabla c_j + u c_j, \tag{1}$$

where the spatial distances x and y are normalized by L, $D_j = D_j^*/D_1$, $c_j = c_j^*/c_{1\infty}$ $\Phi = F\Phi^*/RT$, $u = u^*L/D_1$ and $N_j = N_j^* L/(D_1 c_{1\infty})$. The starred quantities are dimensional. The fluid velocity u is given by Wang et al. (1994). If the origin is attached to the center of the electrode on the moving plate and if $L/B \ll 1$, the dimensionless velocity parallel to the electrode can be approximated by

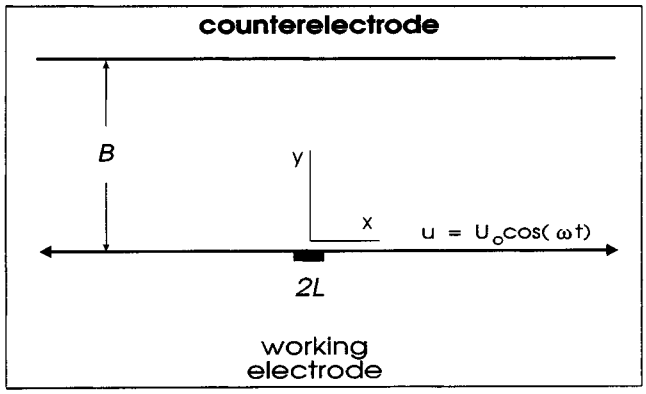

Figure 1. Electrochemical cell.

The working electrode is flush mounted in an otherwise insulating plate. Mixing is induced by an in-plane sinusoidal motion of the plate.

$$u = Pe\, y \cos(\tau), \tag{2}$$

where $\tau = \omega t - \theta$, where θ is a constant. The Peclet number is given approximately by

$$Pe = \sqrt{\frac{\omega}{\upsilon}}\,\frac{U_0 L^2}{D_1^*}. \tag{3}$$

It is assumed that no homogeneous reactions take place in the solution; hence the M (one for each species) material balance equations in dimensionless terms become

$$\Omega \frac{\partial c_j}{\partial \tau} = - \nabla \cdot N_j, \tag{4}$$

where $\Omega = (\omega L^2/D_1^*)$. The electroneutrality constraint is also imposed (Newman, 1991):

$$\Sigma z_j c_j = 0. \tag{5}$$

Boundary conditions

At the outer boundary away from the electrode, $c_{j\infty} = 1$ and Φ is arbitrarily set to zero. At $y = 0$, the boundary conditions are $N_j = 0$ at the insulating wall for all species j. A zero-flux condition is also imposed on the electrode for all species except the reactants and products. A kinetic expression relating the surface concentration and potential to the reactant and product fluxes is also imposed at the electrode. In the case of copper deposition, the boundary condition can be written as (Mattsson and Bockris, 1959):

$$i = \frac{F z_1 c_{1\infty} D_1^*}{L} N_1 = i_0 \{\exp[\alpha(V - \Phi)] - c_1^{\gamma} \exp[-\beta(V - \Phi)]\}, \tag{6}$$

where i_0 is the exchange current density, α and β are transfer coefficients, V is the dimensionless electrode potential.

Equations 1, 4, 5, and the boundary conditions define a nonlinear and coupled system of partial differential equations. In the next section, a control-volume method is described for the numerical solution.

Numerical Method

A control-volume formulation was applied to the set of coupled partial differential equations (Patankar, 1980). The equations were linearized around a guessed value. The guessed values were updated iteratively to convergence before executing the next time step. Since the electroneutrality constraint tightly couples the potential and concentration fields, the discretized set of algebraic equations at each node point were solved simultaneously. Either point-by-point or line-by-line overrelaxation methods were used to solve the algebraic equations. An overrelaxation parameter of 1.5–1.8 was typically used. The two methods required similar computational times. An upwind scheme was used for all variables for high-Pe problems, while a central-difference scheme was

used for low *Pe* (Patankar, 1980). In some trial simulations, a central-difference scheme was used for the potential for high-*Pe* problems, but no appreciable differences in the results were observed.

Numerical experiments were performed to determine the minimum computational domain and an adequate grid size as described by Wang et al. (1994). Uniform grids were used near the electrode. Beyond this region, nonuniform grids, with a stretching factor of less than 1.2 in both directions, were used. When the electrical field is large, a more finely resolved grid was necessary. The number of iterations to obtain a converged result was also found to increase in the presence of large electric fields. The convergence rate was improved if a good trial solution was given to the potential. However, convergence was obtained for almost any initial guess.

Effect of Migration on Mass-transfer-limited Current Densities

At the limiting current, the electrode-kinetics boundary condition can be replaced with a condition that $c_r = 0$ at the surface, where c_r is the concentration of the limiting reactant. The supporting electrolyte changes the magnitude of the limiting current because the extra ionic strength increases solution conductivity, which reduces the electrical field. Electrical-migration effects on limiting currents have been treated by Newman (1967, 1991) for several problems, including the rotating disk, the stagnant diffusion layer, and boundary-layer flows. The ratio of the limiting current density i_L to the limiting current density i_D computed by neglecting migration is a measure of the effect of migration. An interesting result from boundary-layer analysis is that the migration enhancement i_L/i_D is the same for all positions along the electrode. The same result is found for a stagnant electrolyte, but has not been established for all flow conditions.

The effect of migration on limiting currents was studied as a benchmark of the numerical code and to test the limits of the boundary-layer analysis. Two chemistries are considered (both in the presence of an oscillating or steady shear flow):

1. Depositing copper ions from a $CuSO_4/H_2SO_4$ solution
2. Reducing hydrogen ions from an HCl/KCl solution.

It is assumed that H_2SO_4 completely dissociates to H^+ and sulfate ions. This is a good assumption for the case of little supporting electrolyte (see experimental section), and is not a significant source of error for the case of excess supporting electrolyte. The ratio of supporting electrolyte to reactant concentrations was varied in the simulations, and the infinite-dilution values for diffusion coefficients tabulated by Newman (1991) were used. The simulation parameters are summarized in Table 1.

The mass-transfer-limited dimensionless flux for copper deposition is shown in Figure 2 for two values of supporting electrolyte concentration and two values of *Pe*. Results are shown for a steady shear flow (from left to right). The amount of supporting electrolyte is represented by the ratio r, defined to be c_3/c_2 for case 1 and $c_3/(2c_2)$ for case 2. When $r = 0$, we have a binary electrolyte. Here and for all other simulations of steady shear flow, it was found that the magnitude of the current density increased by a constant, multiplicative factor i_L/i_D, but that the normalized current distribution does not change. In other words, the $\sqrt{r} = 0.3$ results

Table 1. Simulation Parameters

No.	Species	$D_j \times 10^5$ cm^2/s	z_j
	Case 1		
1	Cu^{2+}	0.72	2
2	SO_4^{2-}	1.065	−2
3	H^+	9.312	1
	Case 2		
1	H^+	9.312	1
2	Cl^-	2.032	−1
3	K^+	1.957	1

can be obtained by multiplying the current distribution in the presence of excess supporting electrolyte by a constant.

In Figure 3, the effect of *Pe* number on the multiplicative constant for $\sqrt{r} = 0.3$ is shown. The dashed line at small *Pe* number is the value given by the case of no convection (Newman, 1991), and the dashed lines at large *Pe* are the asymptotic limits predicted from boundary-layer analysis (Newman, 1967). When $Pe > 1$, the i_L/i_D approach the high-*Pe* limits. The simulation also agrees with theory when $Pe \to 0$. The constant i_L/i_D is a function of *Pe* when the diffusion coefficient D_1 of the reacting ion is considerably different from D_2, as in the case of proton reduction.

When $r = 0$, theoretical expressions for i_L/i_D can be derived because of the well-known (Newman, 1991) simplifications possible for binary electrolytes. The results help explain why the migration enhancement is only weakly dependent on *Pe*, except when the reactant is much more mobile than the counterion. When only the cation reacts at the surface, the constant i_L/i_D is given by

$$\frac{i_L}{i_D} = \frac{z_1 - z_2}{|z_2|} \qquad \text{(when } r = 0,\ Pe = 0\text{)}. \tag{7}$$

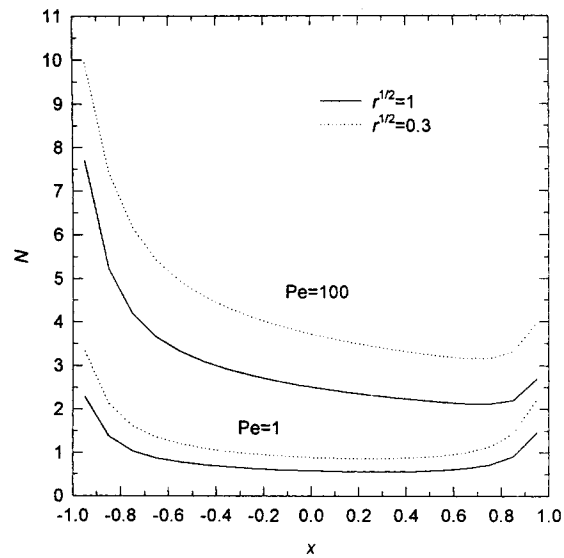

Figure 2. Mass-transfer-limited dimensionless flux for copper deposition in the presence of a steady, shear flow.

The leading edge of the electrode is positioned at a dimensionless distance of −1.

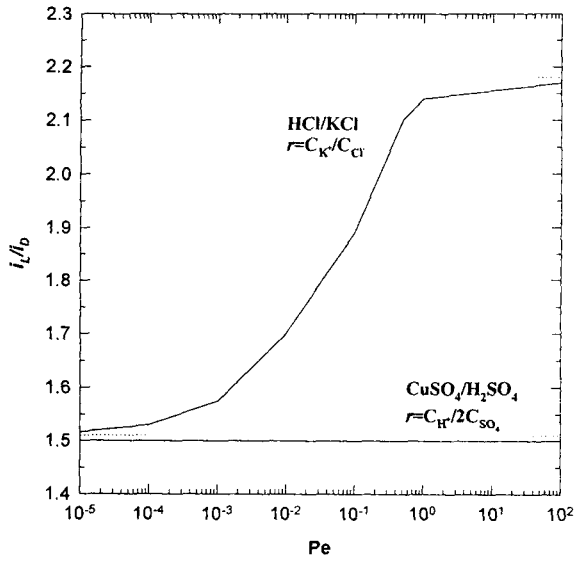

Figure 3. Effect of *Pe* number on the multiplicative constant i_L/i_D in the presence of a steady shear flow for $\sqrt{r} = 0.3$.

The three dashed lines are asymptotic predictions for small and large *Pe*.

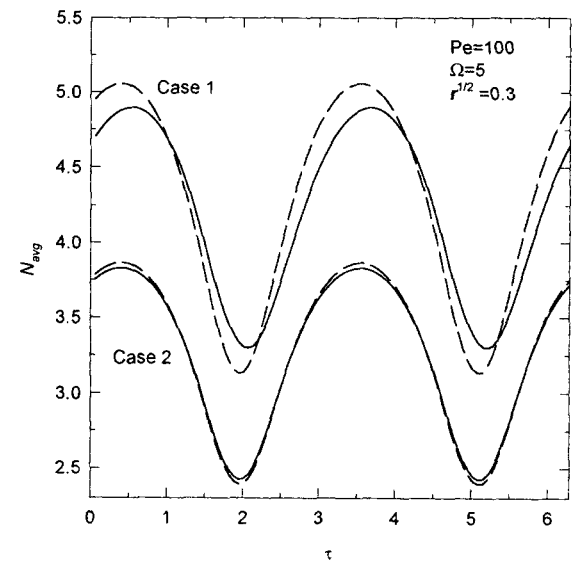

Figure 4. Effect of electrical migration in the presence of an unsteady, periodic shear flow.

The solid lines are simulation results, and the dashed lines are constant multiplicative factors of the excess-supporting-electrolyte simulations. (Case 1: proton reduction; case 2: copper deposition.)

Interestingly, the enhancement is independent of the values of the diffusion coefficients. For a steady shear flow, the constant i_L/i_D is given by

$$\frac{i_L}{i_D} = \frac{z_1 - z_2}{|z_2|}\left(\frac{z_1(D_1/D_2) - z_2}{z_1 - z_2}\right)^{1/3} \quad \text{(when } r = 0,\ Pe \to \infty\text{)}. \quad (8)$$

A comparison of Eqs. 7 and 8 indicates that the effect of *Pe* on i_L/i_D for copper deposition (where $D_1/D_2 = 0.7$) might be negligible.

The factor i_L/i_D for copper deposition was also found to be independent of the flow conditions for the unsteady shear flow. Furthermore, the enhancement factor was largely independent of position and time. However, the time-averaged enhancement factor was weakly dependent on position for some values of *Pe* and Ω for proton-reduction simulations. For all values of *Pe*, the enhancement factor based on the time and spatial average current densities was found to decrease with increasing Ω.

Figure 4 shows the spatial average current density as a function of time for $\sqrt{r} = 0.3$. The bottom curves are results for copper deposition and the top curves show results for proton reduction. For both sets of curves, the solid lines are simulation results. The dashed lines are obtained by multiplying the $r = 1$ result by a constant. Time independence of the enhancement factor would imply that the curves lie on top of one another. This is seen for the copper-deposition curves. The slight discrepancies are believed to be numerical and are not physically significant.

For the proton-reduction case, the amplitude of the oscillations is slightly less than expected from multiplying the excess-supporting-electrolyte results by a constant. Also, the simulations are out of phase with the excess-supporting electrolyte simulations. The phase lag is the result of the supporting electrolyte being significantly less mobile than the reacting hydrogen ion. This results in an electric field, which is coupled to all of the concentration fields, that lags behind the concentration field of the hydrogen ions.

Experimental Apparatus and Procedure

Flow cell

All experiments used an electrolyte composed of 3-mM cupric sulfate and either 0.1 M or 0.3 mM sulfuric acid. The working electrode was made of 99.999% copper sheet of thickness $2L = 0.025$ cm and a length of 2 cm. It was mounted in a thermoplastic resin cast in a cylindrical mode. The top of the mold was cut flat to expose a fresh metal surface, which was polished down to 600 grit, followed by 0.3-μm polishing alumina. The working-electrode assembly, with the line electrode perpendicular to the fluid flow, was flush mounted in a hole near the center of the moving plate. More details of the setup can be found in DeBecker et al. (1995a). A thin 20× 13-cm copper counterelectrode was mounted on the wall (at a distance $B = 1.6$ cm) opposite the working electrode. A Hg/Hg_2SO_4 reference electrode was placed very far (compared to L) from the working electrode.

A Pine AFRDE4 potentiostat was used to control potential and measure current, and a Lucas-Schaevitz linear variable differential transformer was used to measure the position of the moving plate. A LPCLAB DT-2811 A/D board was connected to a computer to record applied potential, plate position, and current as functions of time.

Experiments were performed potentiostatically in a deaerated electrolyte. A thin layer of copper was deposited on the working electrode at low overpotentials before the collection of experimental data. The electrical potential was decreased from equilibrium by increments of 20 mV until a limiting cur-

rent was reached. The electrode was then polished and treated to have a fresh surface for the next set of experiments.

Rotating-disk electrode

A copper rotating-disk electrode (RDE) was fabricated out of a 0.9-cm-diameter rod with the same purity as the line electrode. It was encased in a cylindrical thermoplastic mold with outer diameter 1.9 cm. The electrode was polished and treated the same way as the line. It was then connected to a Pine Instruments RDE setup. The solution was sparged with nitrogen for at least one hour. Experiments were performed potentiodynamically with a scan rate of 5 mV/s. Polarization curves were obtained at several rotation speeds. The electrodes were polished before every change of rotation speed.

Simulation Parameters for Comparison with Experiment

Below the limiting current, the electrode boundary condition must be modified. For a kinetic relationship given by Eq. 1, there are four parameters: i_0, α, β, and γ. The following were determined previously (Mattsson and Bockris, 1959): $\gamma = 0.5$, $\alpha = 1.5$, and $\beta = 0.5$. The exchange current density i_0 was determined from RDE experiments. Figure 5 shows simulated and experimental polarization curves on an RDE for deposition from a 3-mM $CuSO_4$ and 0.1-M H_2SO_4 solution. The ohmic drop, estimated with AC impedance, was subtracted from the applied potential to estimate surface overpotential. Simulations were fit to experiments to obtain $i_0 = 0.4$ mA/cm^2.

Newman (1991) shows that seven dimensionless parameters are needed for the analysis of one reaction occurring on an RDE. Once the chemistry is specified, the number of parameters that need to be investigated in a design analysis can be greatly reduced. For example, the kinetic parameters α, β, γ, and to a lesser extent i_0 are fixed by the chemical reactions of the process and may not be a design consideration.

Often, the parameters considered in design are the fraction of the limiting current density i_{avg}/i_L and the ratio of the ohmic-to-kinetic resistances. The value of i_L depends on the amount of supporting electrolyte r and on the degree of mixing in the cell. On the rotating disk, i_L depends on rotation speed, and in the oscillating-flow cell, i_L is a function of Pe and Ω. Equation 3 indicates that Pe depends on the size of the electrode, so that for a given shear stress at the wall, i_L changes with size. The ohmic resistance also depends on cell size and r. For the present example, the ohmic resistance relative to the kinetic resistance is given by the linear and the Tafel Wagner numbers, Wa_L, and Wa_T:

$$Wa_L = \frac{RT\kappa}{F(\alpha + \beta)Li_0}$$

$$Wa_T = \frac{RT\kappa}{F\beta L\,|\,i_{avg}\,|}.$$

Comparison of Experiment to Simulation

Temporal variations of the spatial average of the current density are shown in Figure 6 for the case of excess supporting electrolyte and in Figure 7 for $\sqrt{r} = 0.3$. The experimental points and the simulated dashed lines are in agreement. In both cases, nearly two complete periods ($\tau = 2\pi$) of steady, periodic results are shown. In Figure 6, the top curves labeled $V = -0.47$ V corresponds to 57% of the limiting current, and the curve labeled $V = -0.55$ V corresponds to 93% of the limiting current. In Figure 7, the top curve is at 45% and the bottom curve is at 97% of the limiting current. As expected, the magnitude of the oscillations in the current density increases as i_{avg}/i_L increases.

A large number of simulations and experiments can be summarized with a polarization curve, which gives the time-

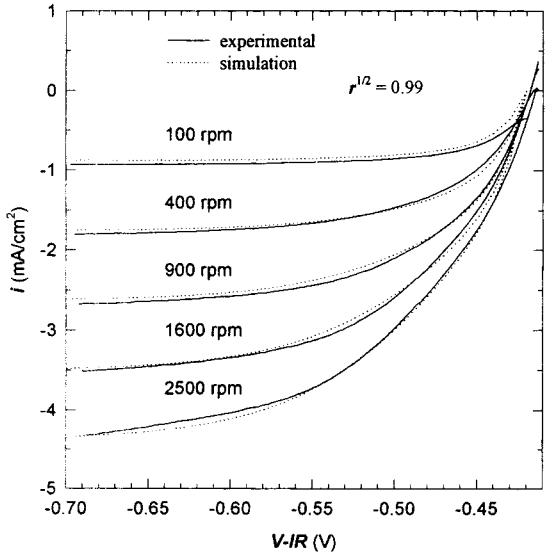

Figure 5. Polarization curves on a RDE for copper deposition with 3-mM copper sulfate and 0.1 M sulfuric acid.

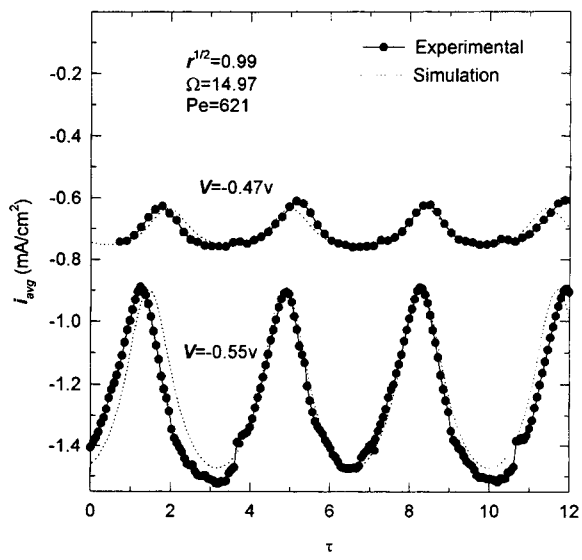

Figure 6. Temporal variation of the spatial average of the current density with 3-mM copper sulfate and $\sqrt{r} = 0.99$ in sulfuric acid solution.

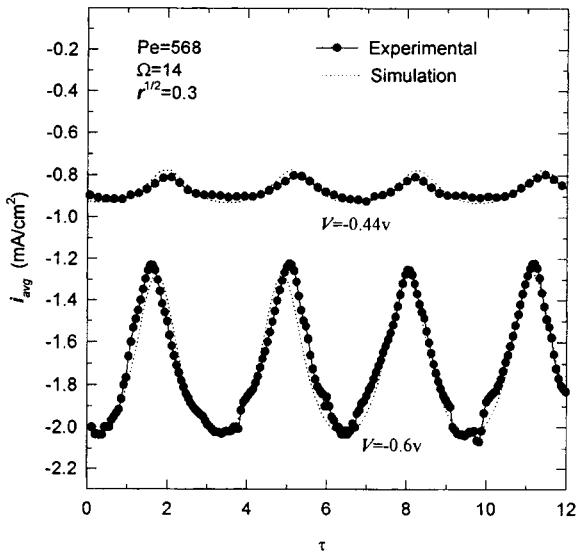

Figure 7. Temporal variation of the spatial average of the current density with 3-mM copper sulfate and $\sqrt{r} = 0.3$ in sulfuric acid solution.

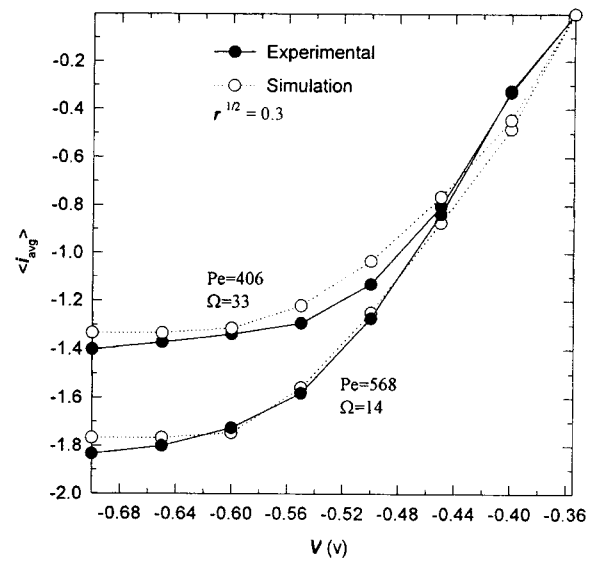

Figure 9. Time-averaged polarization curves in the oscillating-flow cell for copper deposition with 3-mM copper sulfate and $\sqrt{r} = 0.3$ in sulfuric acid solution.

averaged current density vs. applied potential. Figure 8 shows such curves for $\sqrt{r} = 0.99$, and Figure 9 gives them for $\sqrt{r} = 0.3$. Here $\langle i_{avg} \rangle$ is the time average of the spatial average of the current density. For each point in the figures, only the quasi-steady result, after the initial transients disappeared, was reported. The time average was taken over at least five periods.

As predicted by simulation, as the concentration of supporting electrolyte was decreased, the limiting current density increases. Without adjusting any parameters obtained from the RDE, the simulation results for the oscillating-flow cell match the experimental results reasonably well. The discrepancies for $\sqrt{r} = 0.99$ on the limiting current are believed to be due to changes in the surface finish. Previous characterization of the cell with a redox couple (DeBecker et al., 1995a) suggest that, for this range of Pe and Ω, discrepancies due to nonidealities in fluid flow should be less than 3%.

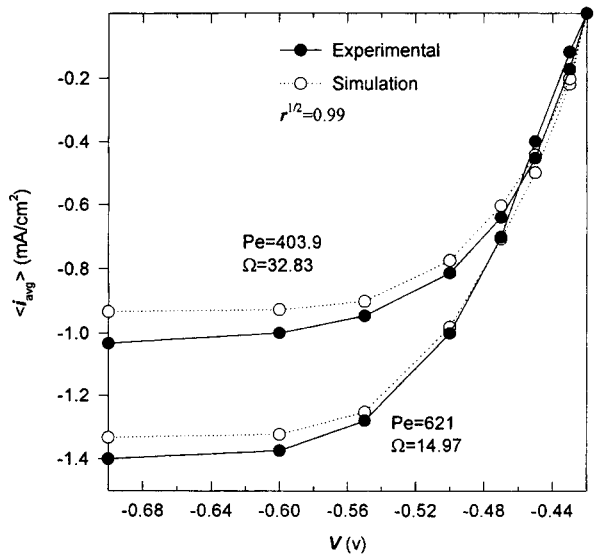

Figure 8. Time-averaged polarization curves in the oscillating-flow cell for copper deposition with 3-mM copper sulfate and $\sqrt{r} = 0.99$ in sulfuric acid solution.

Current distribution

The scaling of the current distribution with size is of fundamental concern in process design, but can be somewhat difficult to predict without the aid of simulations because the Wagner numbers are inversely proportional to size and, for this case, because the limiting current density $i_L \propto L^{-1/3}$. Figure 10 shows the effect of the electrode half-length L on the current distribution for two different amounts of supporting electrolyte. Here, a steady flow with a shear of 20 s^{-1} and an average current density of -46 mA/cm^2 are assumed. The kinetic parameters and transport properties for the copper-deposition experiments were used.

For both cases, the current distribution becomes more uniform as L decreases. The reasons for the increased uniformity are that the ohmic and mass-transfer resistances both decrease. For $L = 1$ results, the $\sqrt{r} = 0.71$ curve looks similar to a mass-transfer-limited current distribution. In contrast, the $\sqrt{r} = 0.3$ curve resembles more closely a secondary-current distribution (Newman, 1991). The reason for this is that solution conductivity is significantly lower for the latter case, causing the ohmic resistance to become as, or more, important than the mass-transfer resistance.

Conclusions

Tertiary-current-distribution solvers, which are time accurate and based on a control-volume formulation, can be effectively implemented if the tight coupling between the electrical and concentration fields is realized. Numerical simula-

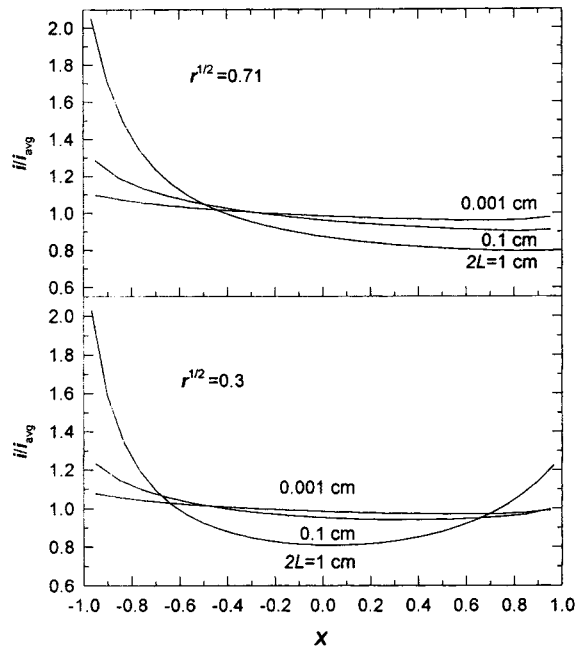

Figure 10. Effect of electrode size on the current distribution in the presence of a steady shear flow for two different amounts of supporting electrolyte.

Transport and kinetic parameters are given in the text. For all cases, the average current density is -46 mA/cm^2 and the shear is 20 s^{-1}.

tions show the electric-field enhancement of limiting currents in the presence of a steady, shear flow agree with boundary-layer analysis when *Pe* is on the order of 10 or higher. The present analysis also elucidates for steady and unsteady shear flows that the electric-field enhancement is a weak function of *Pe* unless the ratio of the mobilities of the reacting and counterions are significantly different from one. Experimental results on copper deposition agree with simulations, indicating, at least for relatively simple electrode kinetics, that measurements from a rotating disk electrode coupled with numerical modeling can predict behavior in other geometries without need to adjust parameters.

Acknowledgments

This work was supported by the National Science Foundation under grant CTS-93-15991.

Notation

D_j^* = diffusion coefficient of species j, cm^2/s
D_j = dimensionless diffusion coefficient of species j
F = Faraday's constant, 96,487 C/mol
i_{avg} = spatial average current density, mA/cm^2
N_{avg} = average dimensionless flux
t = time, s
U_0 = amplitude of plate velocity, cm/s
x,y = dimensionless Cartesian coordinate
z_j = charge number of species j
α = anodic transport number
β = cathodic transport number
γ = kinetic concentration exponent
Φ = dimensionless potential
θ = phase shift for the shear, rad
κ = solution conductivity
τ = dimensionless time
Ω = dimensionless frequency

Literature Cited

Alavyoon, F., "Unsteady Natural Convection and Mass Transfer in Copper Electrolysis with a Supporting Electrolyte," *Electrochim. Acta*, **37**, 334 (1992).

Alkire, R., and A. A. Miraferi, "The Current Distribution Within Tubular Electrodes under Laminar Flow," *J. Electrochem. Soc.*, **120**, 1507 (1973).

Alkire, R., and A. A. Miraferi, "Current Distribution in a Tubular Electrode under Laminar Flow: One Electrode Reaction," *J. Electrochem. Soc.*, **124**, 1043 (1977a).

Alkire, R., and A. A. Miraferi, "Current Distribution in a Tubular Electrode under Laminar Flow: Two Electrode Reactions," *J. Electrochem. Soc.*, **124**, 1214 (1977b).

Baker, D., M. W. Verbrugge, and J. Newman, "A Transformation for the Treatment of Diffusion and Migration. Application to Stationary Disk and Hemisphere Electrodes," *J. Electroanal. Chem.*, **314**, 23 (1991).

DeBecker, B., P. Duby, V. Modi, and A. C. West, "Mass Transfer to a Line Electrode in Presence of a Periodic Fluid Flow," *J. Electrochem. Soc.*, **142**, 3001 (1995a).

DeBecker, B., D. Yang, P. Duby, V. Modi, and A. C. West, "Mass Transfer Current Distributions on Electrode Arrays in the Presence of a Shear Flow," *J. Electrochem. Soc.*, **142**, 3413 (1995b).

Dukovic, J., "Feature-scale Simulation of Resist-patterned Electrodeposition," *IBM J. Res. Develop.*, **37**, 125 (1993).

Engelman, M., "FIDAP Users Manual," Rev. 3, Fluid Dynamics International, Evanston, IL (1986).

Harb, J. N., and R. C. Alkire, "Transport and Reaction during Pitting Corrosion of Ni in 0.5M NaCl: I. Stagnant Fluid," *J. Electrochem. Soc.*, **138**, 2594 (1991a).

Harb, J. N., and R. C. Alkire, "Transport and Reaction during Pitting Corrosion of Ni in 0.5M NaCl: II. Flowing Fluid," *J. Electrochem. Soc.*, **138**, 3568 (1991b).

Law, C., Jr., and J. Newman, "Corrosion of a Rotating Iron Disk in Lamilar, Transition, and Fully Developed Turbulent Flow," *J. Electrochem. Soc.*, **133**, 37 (1986).

Mattsson, E., and J. O'M. Bockris, "Galvanostatic Studies of the Kinetics of Deposition and Dissolution in the Copper + Copper Sulfate System," *Trans. Farad. Soc.*, **55**, 1586 (1959).

Newman, J., "Current Distribution on a Rotating Disk below the Limiting Current," *J. Electrochem. Soc.*, **113**, 1235 (1966).

Newman, J., "The Effect of Migration in Laminar Diffusion Layers," *Int. J. Heat Mass Transfer*, **10**, 983 (1967).

Newman, J., "Engineering Design of Electrochemical Systems," *Ind. Eng. Chem.*, **60**, 12 (1968).

Newman, J., *Electrochemical Systems*, 2nd ed., Prentice Hall, Englewood Cliffs, NJ (1991).

Orazen, M., and M. Miller, "The Distribution of Current and Formation of Salt Film on an Iron Disk below the Passivation Potential," *J. Electrochem. Soc.*, **134**, 392 (1987).

Parish, W. R., and J. Newman, "Current Distribution on a Plane Electrode below the Limiting Current," *J. Electrochem. Soc.*, **116**, 169 (1969).

Parish, W. R., and J. Newman, "Current Distributions on Plane, Parallel Electrodes in Channel Flow," *Electrochem. Soc.*, **117**, 43 (1970).

Patankar, S. V., *Numerical Heat Transfer and Fluid Flow*, McGraw-Hill, New York (1980).

Pesco, A. M., and H. Y. Cheh, "The Current Distribution within Plated Through-Holes," *J. Electrochem. Soc.*, **136**, 399 (1989).

Pillay, B., and J. Newman, "Modeling Diffusion and Migration in Dilute Electrochemical Systems Using the Quasi-Potential Transformation," *J. Electrochem. Soc.*, **140**, 414 (1993).

Vahdat, N., and J. Newman, "Corrosion of an Iron Rotating Disk," *J. Electrochem. Soc.*, **120**, 1682 (1973).

Wang, X., V. Modi, and A. C. West, "Limiting Current Density on a Line Electrode in the Presence of a Tangential, Oscillating Fluid Flow," *J. Electrochem. Soc.*, **141**, 2753 (1994).

Manuscript received May 20, 1996, and revision received Aug. 26, 1996.